The Astrophysical Journal, 709:1–5, 2010 ??? doi:10.1088/0004-637X/709/1/1

PHOTODISSOCIATION DYNAMICS OF METHYLAMINE CATION AND ITS RELEVANCE TO TITAN'S IONOSPHERE

Prashant Chandra Singh, Lei Shen, Jia Zhou, H. Bernhard Schlegel, and Arthur G. Suits
Department of Chemistry, Wayne State University, Detroit, MI, 48202, USA; asuits@chem.wayne.edu
Received 2009 November 12; accepted 2009 December 8; published 2010 ???

ABSTRACT

Photodissociation of $CH_3NH_2^+$ has been studied using the DC sliced ion imaging technique and ab initio calculations in order to understand the formation of $HCNH^+$, an important molecule in Titan's ionosphere. Our experimental and theoretical observations show that hydrogen loss from $CH_3NH_2^+$ has two channels: one giving rise to the triplet species CH_3NH^+, while the other product is $CH_2NH_2^+$. The latter then decomposes further to form $HCNH^+$. H_2 loss from $CH_3NH_2^+$ has only one channel, yielding CH_2NH^+. This species further loses H to form $HCNH^+$. The branching ratio of the H, H_2, and H+H_2 loss channels is found to be 4.2:1:2.5. This is ascribed to the fact that, at these energies, the H loss has one stable triplet product channel, while most of the H_2 loss product further decomposes to $HCNH^+$.

Key words: astrochemistry – ISM: clouds – planets and satellites: general – planets and satellites: individual (Saturn, Titan)

Online-only material: color figure

INTRODUCTION

Titan's dense atmosphere is composed primarily of nitrogen and methane, while less abundant hydrocarbons and nitriles (<ppm) are generated from electron impact and photochemistry involving these major components (Kuiper 1944; Hanel et al. 1981; Yung & Demore 1999). The neutral hydrocarbons and nitriles are then ionized by solar radiation and plasma to create the ionosphere at an altitude of 800 km (Keller et al. 1992) and above. The ionosphere not only plays a crucial role in the chemical and thermal balance of the upper atmosphere, but also establishes a link between Saturn's magnetosphere and neutral atmosphere of Titan (Wilson & Atreya 2004). It may play a central role in the formation of Titan's notorious aerosol haze (Wilson & Atreya 2003).

The *Voyager 1* mission in 1980 (Bird et al. 1997) was the first attempt to experimentally study the ionosphere in Titan, more recently extended by the Cassini/Huygens mission in 2005 (Wahuland et al. 2005; Waite et al. 2005). Cassini has performed the first in situ measurements of the environment of Titan's ionosphere with the ion and neutral mass spectrometer (INMS) experiment. Cassini also reported the surprising observation of very large anions in the upper atmosphere at an altitude of 900 km and above, but this is not the subject of the present investigation. Apart from these measurements, there are many other laboratory-based studies (Anicich et al. 2003; Anicich & McEwan 2006) and models (Carrasco et al. 2007, 2008; Vervack et al. 2004; Galand et al. 1999) that have been reported in the literature to explore the nature of the ionosphere. These studies indicate that a description of Titan's ion chemistry is crucial for our understanding not only of Titan's upper atmosphere but also of the aerosol formation process in general. In Titan's environment, major neutral species N_2 and CH_4 are ionized by solar radiation and plasma producing N_2^+, N^+, CH_4^+, CH_3^+, CH_2^+, and CH^+ ionic species, which further convert into higher mass compounds through complicated ion-neutral chemistry. Cassini's INMS shows the presence of a total of 45 different ions in Titan's ionosphere, with $m/z = 28$ as the most abundant ion. Further analysis of the data identified the mass 28 principally as $HCNH^+$ ion, consistent with the theoretical model (Cravens et al. 2006). After these missions, several experimental and theoretical studies have been performed showing the importance of $HCNH^+$ in many ion-neutral reactions, including those in Titan's ionosphere (Cui et al. 2009; Vuitton et al. 2007).

Apart from the $m/z = 28$ peak, there are several peaks such as $m/z = 30$, 18, and 66 that have also been found from the INMS for which assignment is still a matter of dispute. Recently, Vuitton et al. proposed that most of these new peaks are due to the reaction of the major species with several nitrile species whose abundance is low. They assigned the $m/z = 30$ peak as $CH_2NH_2^+$ (Vuitton et al. 2006a, 2006b). $CH_2NH_2^+$ is also an important species which has been found in the interstellar medium, and its role in astrobiology has been discussed in detail by the Kaiser group (Gu et al. 2009). Another important amine species is CH_3NH_2, which actually has been detected in the interstellar medium toward Sgr B2 and Ori A in its 5_{15}–5_{06} (73.0 GHz), and 4_{14}–4_{04} (86.1 GHz) transitions (Kaifu et al. 1975); however, the formation pathway has not been confirmed in laboratory studies.

These studies show the importance of $HCNH^+$, $CH_2NH_2^+$, and $CH_3NH_2^+$ in Titan's ionosphere and in the interstellar medium, and suggest its potential role in many ion-neutral reactions and astrobiology. However, there are no laboratory studies to date which can give systematic information about the nature of the reaction dynamics and formation mechanisms for these species. It is surprising that $HCNH^+$ and $CH_2NH_2^+$ have been detected in Titan's environment, but until now no CH_2NH^+ has been reported there. In order to understand the pathways involved in the formation of the $HCNH^+$, we have studied the photodissociation of the $CH_3NH_2^+$ cation using ab initio calculations and DC sliced ion imaging methods. It is worth mentioning here that although $CH_3NH_2^+$ has not been detected in the Titan's ionosphere yet, it is a good source for the formation of $HCNH^+$ and also provides the pathway to understand the ion–molecule reactions related to formation and reactions of $HCNH^+$.

EXPERIMENT

The detailed description of the experimental setup used in this study has been reported elsewhere (Leskiw et al. 2005),

and only a brief sketch is given here. A pulsed molecular beam of methylamine (Linde, CP Grade, 99.5%) is made by supersonic jet expansion of a mixture of approximately 10% of methylamine in an argon carrier gas at a backing pressure of 2 bar from a pulsed nozzle valve (General Valve series 9) into the source chamber of the differentially pumped apparatus. After passing through a 1 mm diameter skimmer located 3.8 cm downstream of the pulsed nozzle orifice, the supersonic molecular beam enters into a velocity mapping ion optics assembly consisting of four electrodes. A laser beam tuned to a one-photon resonant excitation of methylamine perpendicularly intersects the molecular beam in the main chamber. The operating pressures were maintained at 1.0×10^{-5} torr in the source chamber and at 5.0×10^{-8} torr in the main chamber.

The ultraviolet light used here was generated by frequency doubling of the output of a tunable OPO laser (Spectra-Physics MOPO-HF) pumped by the third harmonic of a seeded neodymium-doped yttrium aluminum garnet (Nd:YAG) laser. The laser beam was vertically polarized, parallel to the detector surface, and then was focused with a 20 cm focal length lens into the interaction region. Typical output power for the pulsed laser beam entering into the chamber was 0.3–0.5 mJ pulse^{-1}. Wavelength calibration was achieved using a wavemeter (coherent wave-master). In these experiments, a single color laser was used to ionize the CH_3NH_2 and to photodissociate the resulting $CH_3NH_2^+$ ions. State selected $CH_3NH_2^+$ were created using a one-color resonance-enhanced two-photon ionization technique at 41,690 cm^{-1} (150 kcal mol^{-1}) after which a third photon gives rise to photofragmentation. Both ionization and dissociation occurred from the same laser pulse. These experiments were performed at relatively low power, where it is assumed that photofragmentation takes place due to absorption of a single photon. However, the possibility of a multiphoton dissociation process in the cation is not ruled out. After ionization and dissociation, the photofragments were accelerated through the multi-lens velocity mapping assembly. Time of flight mass separation occurred along an 80 cm length flight tube after which the mass separated ions impacted a position sensitive dual MCP/P-47 phosphor screen of 120 mm diameter (Burle/Photonis). The resulting images were recorded using a CCD camera (Sony XT-ST50) in conjunction with the IMACQ megapixel acquisition software developed by our group (Li et al. 2005), which permitted real-time event counting and centroiding of the data. The central regions of the ion clouds were sliced by gating the detector on for 90 ns. The images were typically accumulated for 40,000 laser shots for each data set. Calibration of our images was achieved on the basis of the experimentally observed images of CO ($v = 0, J = 65$) in the photodissociation of OCS at 230 nm. Total translational energy distributions for the different channels were obtained by integrating the images over angle at each radius, the converting to total translational energy using the IMAN program. The branching ratios between these channels were calculated by integrating the ion counts from their respective images for the same number of shots.

Theoretical Methods

Ab initio methods have been used to calculate the geometries, energies, and vibrational frequencies of the $CH_3NH_2^+$ ion and its photofragmentaion products. All the calculations have been performed using Gaussian 03 (Frisch et al. 2007). The geometries of the minima and transition states for the $CH_3NH_2^+$ parent ion and its photofragments have been optimized using

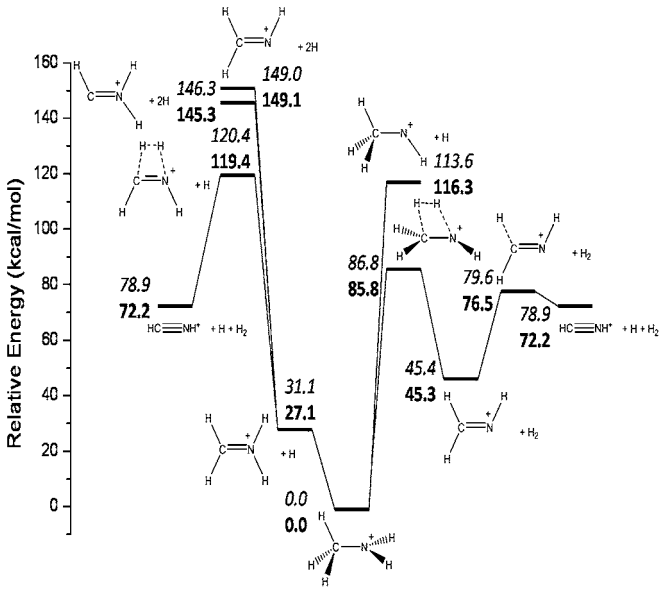

Figure 1. Potential energy profile for the dissociation pathways of $CH_3NH_2^+$. The energy values given in the bold were calculated at the CBS-APNO level of theory while those in italics were calculated at the B3LYP/6–311 $g(d, p)$ level of theory.

B3LYP/6–311G (d, p) and CBS-APNO level of theory, and the vibrational frequency of the optimized structures has been calculated at the same level of theory to confirm the nature of the optimized structures on the potential energy surface. The CBS-APNO complete basis set extrapolation method (Montgomery et al. 1994) has been used to compute accurate energies of the $CH_3NH_2^+$ and its photofragments. The method provides a mean absolute deviation of 0.5 kcal mol^{-1} for heats of formation and is in agreement with B3LYP/6–311G (d, p) calculations having a mean absolute deviation of less than 2.0 kcal mol^{-1}.

RESULTS

To understand the pathways for photodissociation of $CH_3NH_2^+$, the potential energies for photodissociation products of $CH_3NH_2^+$ have been calculated using both the CBS-APNO and B3LYP/6–311G (d, p) level of theories. Figure 1 shows the structures of the relevant minima as well as transition states at both the CBS-APNO and B3LYP/6–311 G (d, p) level of theories. For the $m/z = 30$ (H loss) channel, both CH_3NH^+ and $CH_2NH_2^+$ products are accessible. For the $m/z = 29$ channel, there are two possible pathways: one in which there is direct H_2 molecule loss from the parent, and one in which there are two successive H atom losses. Similarly, the $m/z = 28$ product can arise via two general processes: one in which first one hydrogen atom is lost followed by H_2 molecule loss (H + H_2 loss), or alternatively, H_2 loss followed by H loss (H_2 + H loss). Successive loss of three H atoms is not energetically feasible given the available energy of ~150 kcal mol^{-1}. In the case of the direct H + H_2 or H_2 + H loss from $CH_3NH_2^+$ to form $m/z = 28$, two stable products $HCNH^+$ and CNH_2^+ are possible, while the other product, H_2CN^+, is a transition-state structure. Between the two stable $m/z = 28$ products, only $HCNH^+$ is energetically feasible. For the hydrogen loss channel, both CH_3NH^+ and $CH_2NH_2^+$ products are barrierless processes. The lowest energy CH_3NH^+ is a triplet species, and further dissociation from triplet CH_3NH^+ to singlet $HCNH^+$ is spin forbidden. $CH_2NH_2^+$, another hydrogen loss product, can decompose further to $HCNH^+$

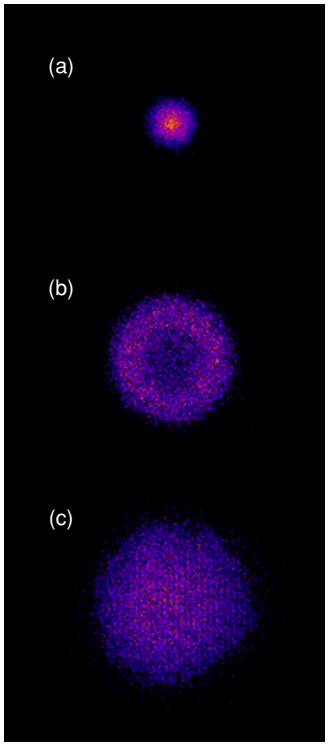

Figure 2. Ion images for (a) $m/z = 30$ (H loss), (b) $m/z = 29$ (H_2 loss), and (c) $m/z = 28$ (H + H_2) loss channels of $CH_3NH_2^+$ at 41690 cm^{-1}.
(A color version of this figure is available in the online journal.)

via the direct H_2 loss, which has a barrier of 118 kcal mol^{-1}. H_2 loss from $CH_3NH_2^+$ can then proceed via two isomeric products CH_2NH^+ and $CHNH_2^+$; the former is 4 kcal mol^{-1} higher in energy than the latter. The H_2 loss from the parent to form the CH_2NH^+ product has a barrier of 86 kcal mol^{-1}; it can further dissociate to $HCNH^+$ over a barrier of 34 kcal mol^{-1}. Efforts to elucidate the other pathway for direct H_2 loss from $CH_3NH_2^+$ to produce $CHNH_2^+$ resulted in the formation of $CH_2NH_2^+$ + H.

Methylamine's REMPI spectrum has mainly a v_9 amine wagging mode progression feature, and it has been extensively studied by Bernstein's group (Taylor & Bernstein 1995). Since methylamine undergoes a large geometry change upon excitation, no origin transition was observed in the REMPI spectrum (Baek et al. 2003a, 2003b). Photofragmentation of the $CH_3NH_2^+$ at 41690 cm^{-1} (5.17 eV) shows mass peaks at the 31, 30, 29, and 28 amu. These fragments are assigned, based on the theoretical calculations, as the parent ion $CH_3NH_2^+$, $CH_2NH_2^+/CH_3NH^+$ from the H loss channel, CH_2NH^+ from the H_2 loss channel, and $HCNH^+$ from the H + H_2 loss channel, respectively.

To get more insight into the photodissociation dynamics of $CH_3NH_2^+$, the DC sliced ion imaging method was used and images and translational energy release were recorded for the photodissociation products of $CH_3NH_2^+$ at 41,690 cm^{-1}. Figure 2 shows the sliced ion images for the H loss (mass 30), H_2 loss (mass 29) and H+H_2 loss (mass 28) produced from the photofragmenation of $CH_3NH_2^+$ at 41,690 cm^{-1}, while Figure 3 shows the total translational energy release for these channels derived from the respective images. The images are similar for all the channels except for the H_2 loss channel where the image has a "hole" inside it. The angular distributions of the fragments are isotropic, which implies of the long lifetime (ps–ns) prior to dissociation. The translational energy release for the hydrogen loss channel has a peak at 0.4 eV and extends to

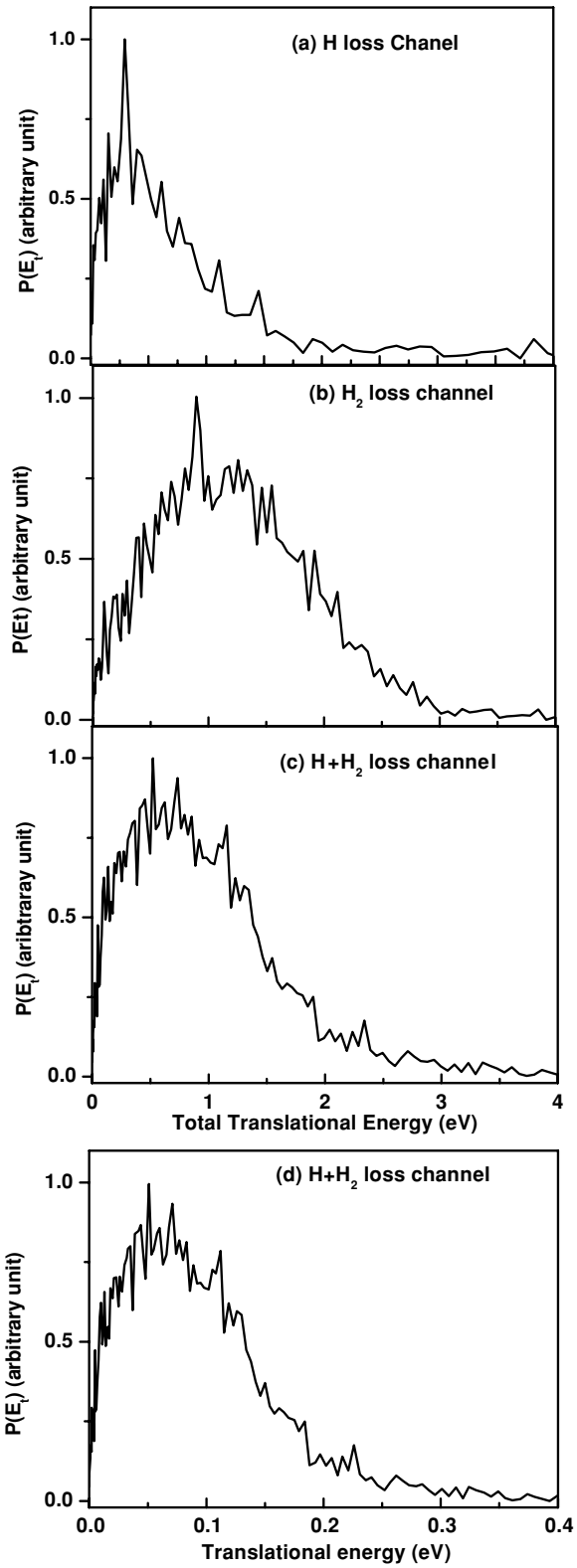

Figure 3. Total translational energy distribution for the (a) $m/z = 30$ (H loss), (b) $m/z = 29$ (H_2 loss), and (c) $m/z = 28$ (H + H_2) loss channels of $CH_3NH_2^+$ at 41690 cm^{-1}, while (d) shows the translational energy for the $m/z = 28$ ($HCNH^+$) product.

2 eV, while for the H_2 loss channel, the peak is at 1 eV and it extends up to 3 eV. Figures 3(c) and (d) show two translational energy release plots for H+H_2 loss (mass 28), in which the first translational energy distribution is derived for cofragment value

of 3 to account for the H+H_2 loss, while the second plot is for the translational energy of the $HCNH^+$ species alone. The branching ratio for these photofragmention channels has been estimated from integration of their respective images and found to be 4.2:1:2.5 (m/z = 30:29:28). The branching ratio for these channels was measured on numerous other transitions from 41,703 cm^{-1} to 43,768 cm^{-1} (corresponding to a wavelength range from 240 to 228 nm), but we found no appreciable change in the branching. In addition, despite a thorough investigation on many transitions in this region, we found no evidence of mode selectivity on the photodissociation dynamics of these ions.

DISCUSSION

For the hydrogen loss channel from $CH_3NH_2^+$, there are two pathways: (1) $CH_2NH_2^+$ + H and (2) CH_3NH^+ + H. The translational energy release for hydrogen loss has maximum value around 0.4 eV and extends to 1.5 eV, which is consistent with the calculations for the CH_3NH^+ + H channel, having maximum available energy of 1.5 eV. The $CH_2NH_2^+$ product has the available energy of 5.1 eV; however, the translational energy release is found to be between 0.1—and 1.5 eV, which likely excludes this as a hydrogen loss product. Rather, the agreement between experimental and theoretical results suggests that CH_3NH^+ is the product detected as the hydrogen loss channel. The other possible product, $CH_2NH_2^+$, can further dissociate to $HCNH^+$ by direct H_2 loss. This mechanism has a barrier of 4.03 eV, which is within the available energy of the primary $CH_2NH_2^+$ product. This suggests that much of the $CH_2NH_2^+$ dissociates further to form $HCNH^+$ + H_2.

The direct H_2 loss from $CH_3NH_2^+$ could have two pathways, one via CH_2NH^+ and the other may be from $CHNH_2^+$. However, theoretical calculation shows that only CH_2NH^+ + H_2 is possible. The H_2 loss image, shown in Figure 2(b) has a hole inside it, and the translational energy release shows that it has maximum around 0.5–1.9 eV while it extends out to 3 eV. This hole in the H_2 loss image, implying the absence of slow fragments, can either correspond to an energy barrier for H_2 loss from $CH_3NH_2^+$ or it can be because of the secondary decomposition of the primary products. The only possible channel for H_2 loss from $CH_3NH_2^+$ is via CH_2NH^+ product formation. This channel has a barrier of 3.7 eV from $CH_3NH_2^+$. This transition state has maximum 2.8 eV available energy from this barrier, which is in nice agreement with the translation energy release plot for H_2 loss shown in Figure 3(b). This strongly suggests that the hole in H_2 loss image is due to the barrier for the H_2 loss from the $CH_3NH_2^+$ to CH_2NH^+. CH_2NH^+ product can dissociate further to $HCNH^+$ + H via a barrier of 1.5 eV. This energy barrier from CH_2NH^+ to $HCNH^+$ is less than the available energy of 2.8 eV, though the available energy depends upon the nature of the exit channel. Even if the decay does not allow the transfer of all excess energy to CH_2NH^+, the 1.7 eV available energy in CH_2NH^+ is enough to overcome the barrier for the formation of the $HCNH^+$ product. Figure 3(c) shows the translational energy for H+H_2 loss, which has a maximum energy around 0.7 eV and extends to 3.0 eV, in good agreement with the maximum available energy for the $HCNH^+$ + H + H_2 product of 3.1 eV. This channel is easily assigned to the $HCNH^+$ product. Figure 3(d) shows the translational energy of $HCNH^+$ alone, which is useful in envisioning the limiting momentum partitioning in this three-body decay process.

The above experimental and theoretical data clearly show that $HCNH^+$ can be formed by two channels from methylamine cation; one is a direct loss of H_2 from $CH_2NH_2^+$ and other is H loss from CH_2NH^+. The H loss channel has two pathways, one is to form CH_3NH^+ in the triplet state and the other product is $CH_2NH_2^+$, which decomposes to $HCNH^+$. Most of the H_2 loss product, CH_2NH^+, finally goes to $HCNH^+$, which is the reason that branching of the H loss is higher than the H_2 loss channels.

Implications for Titan's Atmosphere

We now consider the implications of these results for understanding Titan's atmosphere. The INMS measurements provide details on ion densities in Titan's ionosphere based on the mass-to-charge ratio. Most of the theoretical and experimental efforts in interpreting these data have been directed to chemical identification of these ions. Two main classes of ions in Titan's ionosphere are nitriles and hydrocarbons, and $HCNH^+$ is the most abundant ion. Two possible mechanisms for the formation of nitrogen bearing cations have been discussed in the literature. The first is ion–molecule reactions between N^+ and N_2^+ ions and neutral molecules, while the other possible mechanism involves nitrile protonation. Although there are theoretical models to explain the formation of the nitrogen bearing cations in Titan's ionosphere, there is very little experimental data on ion energetics and photochemistry giving insight into these mechanisms. In view of this, $CH_3NH_2^+$ has been studied as a source to understand possible formation mechanisms and reactive pathways of $HCNH^+$. These results will be helpful for the development of more accurate models in order to understand the formation of the nitrogen bearing cations in Titan's ionosphere. This study also provides the branching ratio between the photodissociation products $HCNH^+$, CH_2NH^+, and $CH_2NH_2^+$. The branching ratio for the formation of the $HCNH^+$ has been estimated earlier for the reactions of C_2Hx^+ with HCN (Mackay et al. 1980) and N^+ with the most abundant contributors (Ascenzi et al. 2001). These branching ratios were determined at the 300 K, and it is very probable that they might be different at the low temperature of Titan's ionosphere.

For detailed modeling of Titan's ionosphere, additional wavelength-dependent data would be useful. As mentioned above, we found little variation of the branching in the range from 218–240 nm. However, based on the potential energy diagram in Figure 1, we can anticipate that at much lower excitation energies, H loss will grow relative to the other decay channels. These and related studies of ion photochemistry can aid in understanding the formation and reactions of key ionic species in Titans upper atmosphere, which may offer insight not only into the chemistry of the ionosphere but also into the chemistry of the haze formation as well.

CONCLUSION

In this paper, DC sliced ion imaging and theoretical studies of $CH_3NH_2^+$ photodissociation have been performed to understand the pathways and branching ratios of different photodissociation product channels. $CH_3NH_2^+$ has been studied as a source to understand the formation of $HCNH^+$ which is the most abundant ion in Titan's upper atmosphere, and to characterize the potential energy surface for reactions leading to $HCNH^+$. Our experimental and theoretical observations show that hydrogen loss from $CH_3NH_2^+$ has two channels, one leading to triplet CH_3NH^+ while other product $CH_2NH_2^+$ decomposes further, to form $HCNH^+$. H_2 loss has only one channel, CH_2NH^+ + H_2, which further loses a hydrogen atom to form $HCNH^+$. The facile decomposition of CH_2NH^+ to $HCNH^+$ may be one of the reasons why no CH_2NH^+ has been observed in Titan's ionosphere. The

branching ratio of the $m/z = 30{:}29{:}28$ is found to be 4.2:1:2.5, which is justified by the fact that the H loss has one stable triplet product channel while most of the H_2 loss product converts to $HCNH^+$.

This work was supported by the National Science Foundation under award numbers CHE-0627854 (AGS) and CHE-0910858 (HBS). We thank Stephanie Everhart for a critical reading of the manuscript.

REFERENCES

Anicich, V. G., & McEwan, M. J. 2006, J. Am. Soc. Mass Spectrom., 17, 544
Anicich, V. G., Wilson, P. F., & McEwan, M. J. 2003, J. Am. Soc. Mass Spectrom., 14, 900
Ascenzi, D., Franceschi, P., Freegarde, T., Tosi, P., & Bassi, D. 2001, Chem. Phys. Lett., 346, 35
Baek, S. J., Choi, K. W., Choi, Y. S., & Kim, S. K. 2003a, J. Chem. Phys., 118, 11026
Baek, S. J., Choi, K. W., Choi, Y. S., & Kim, S. K. 2003b, J. Chem. Phys., 118, 11040
Bird, M. K., Dutta-Roy, R., Asmar, S. W., & Rebold, T. A. 1997, Icarus, 130, 426
Carrasco, N., Alcaraz, C., Dutuit, O., Plessis, S., Thissen, R., Vuitton, V., Yelle, R., & Pernot, P. 2008, Planet. Space Sci, 56, 1644
Carrasco, N., Dutuit, O., Thissen, R., Banaszkiewicz, M., & Pernot, P. 2007, Planet. Space Sci., 55, 141
Cravens, T. E., et al. 2006, J. Geophys. Res., 33, L07105/1
Cui, J., et al. 2008, Icarus, 200, 581
Cui, J., et al. 2009, J. Geophys. Res., 114, A06310/1
Frisch, M. J., et al. 2007, Gaussian Devlopment Version, Revision F.02, (Wallingford, CT: Gaussian, Inc.)
Galand, M., Lilensten, J., Toublanc, D., & Maurice, S. 1999, Icarus, 140, 92
Gu, X., Kaiser, R. I., Mebel, A. M., Kislov, V. V., Klippenstein, S. J., Harding, L. B., Liang, M. C., & Yung, Y. L. 2009, ApJ, 701, 1797
Hanel, R., et al. 1981, Science, 212, 192
Kaifu, N., Takagi, N., & Kojima, T. 1975, ApJ, 198, L85
Keller, C. N., Cravenes, T. E., & Gan, L. 1992, J. Geophys. Res., 97, 12117
Kuiper, G. P. 1944, ApJ, 100, 378
Leskiw, B. D., Kim, M. H., Hall, G. E., & Suits, A. G. 2005, Rev. Sci. Instrum., 76, 104101
Li, W., Chambreau, S. D., Lahankar, S. A., & Suits, A. G. 2005, Rev. Sci. Instrum., 76, 063106
Mackay, G., Vlachos, G., Bohme, D., & Bohme, H. 1980, Int. J. Mass Spectrom. Ion Phys., 36, 259
Montgomery, J. A., Ochterski, J. W., & Peterson, G. A. 1994, J. Chem. Phys., 101, 5900
Taylor, D. P., & Bernstein, E. R. 1995, J. Chem. Phys., 103, 10453
Vervack, R. J., Jr., Sandel, B. R., & Strobel, D. F. 2004, Icarus, 170, 91
Vuitton, V., Doussin, J.-F., Benilan, Y., Raulin, F., & Gazeau, M.-C. 2006a, Icarus, 185, 287
Vuitton, V., Yelle, R. V., & Anicich, V. G. 2006b, ApJ, 647, L175
Vuitton, V., Yelle, R. V., & McEwan, M. J. 2007, Icarus, 191, 722
Wahuland, J.-E., et al. 2005, Science, 308, 986
Waite, J. H., Jr., et al. 2005, Science, 308, 982
Wilson, E. H., & Atreya, S. K. 2003, Planet. Space Sci., 51, 1017
Wilson, E. H., & Atreya, S. K. 2004, J. Geophys. Res., 109, E06002
Yung, Y. L., & Demore, W. B. 1999, Photochemistry of Planetary Atmospheres (Oxford: Oxford Univ. Press)

Reference linking to the original articles

References in pale purple have a clickable link to the original article created from data deposited by its publisher at CrossRef. Any anomalously unlinked references should be checked for accuracy. Blue is used for links to the NASA Astrophysics Data System (ADS) or to e-prints at arXiv.

Online-only colour figures

This proof PDF is identical in specification to the PDF file that will be published in the online journal. To view any online-only color figures as they will appear in the printed journal, we recommend that this color PDF file be printed on a black & white printer.